IEEE Access
Multidisciplinary | Rapid Review | Open Access Journal

Received December 15, 2017, accepted January 23, 2018, date of publication March 23, 2018, date of current version September 5, 2018.

Digital Object Identifier 10.1109/ACCESS.2018.2818884

Monitoring the Smart Grid Incorporating Turbines and Vehicles

MD M. RANA[1], WEI XIANG[1], (Senior Member, IEEE), ERIC WANG[1], AND XUEHUA LI [2]

[1]College of Science and Engineering, James Cook University, Douglas, QLD 4878, Australia
[2]School of Information and Communication Engineering, Beijing Information Science and Technology University, Beijing 100192, China

Corresponding authors: Wei Xiang (wei.xiang@jcu.edu.au) and Xuehua Li (lixuehua@bistu.edu.cn)

This work was supported by the National Natural Sciences Foundation of China under Grant 61628102.

ABSTRACT In contrast to the traditional filtering approaches, this paper presents a message passing algorithm for multi-area interconnected power systems. The interconnected power system incorporating the thermal turbines and electrical vehicles is expressed as a state-space framework. The phasor measurement units are used to obtain the system state information. After receiving the sensing information at the energy management systems, the factor graph based message passing algorithm is developed. This algorithm can estimate the system states in a distributed way considering the Baysian network. Simulation result shows that the developed scheme can be well estimated the system states.

INDEX TERMS Factor graph, interconnected power systems, smart grid, state estimation.

I. INTRODUCTION

Due to fluctuations of load characteristics including sudden changes in the load demand and intermittent of renewable energy generation patterns, the system frequency deviates and oscillates far away from the typical value [1]. Interestingly, the load frequency control (LFC) is able to maintain the system frequencies and interchange powers at the scheduled values by applying suitable control actions [2], [3]. As the system states are unavailable in general, so the state estimation is the first step to design the controller [4]. From the controller design point of view, the detailed procedure for the derivation of a three-phase inverter-based microgrid model including key components and operation modes is described in [5]. The dynamic of the power flow equations are obtained using the Kirchhoff's laws. In order to estimate the system states in a distributed way, the Kalman smoothing filter based state estimation scheme is demonstrated in [6]. In this scenario, it is assumed that nodes can be ordered in space and have access to noisy measurements.

Considerable research has been carried out for the LFC of interconnected power systems. The fractional order observer with a linear quadratic regulator (LQR) is proposed in [7]and [3]. This scheme is only applicable for a continuous-time system, but the discrete-time framework is easy to implement in the digital platforms. The idea is then extended in [8], where a hybrid system is considered. The state estimation algorithm is derived based on continuums-time framework, then discretising the estimation algorithm. Even though, it uses the simple proportional plus integral controller, but the developed algorithm cannot be traced back to the original system. Furthermore, the model predictive control to the LFC of interconnected power systems is presented in [9]. It assumes that the system states are available. Moreover, the Kalman filter based LQR for a network controlled system is proposed in [4]. In fact, the belief propagation based smart grid state estimation for power systems/microgrids is explored in [10]–[12], [30]. Driven by aforementioned motivations, this paper presents a message passing algorithm for multi-area interconnected power systems. The main contributions of the paper are summarized as follows:

- To develop a linearized state-space model of a realistic multi-area interconnected power system considering thermal turbines and electrical vehicles. Each area is interconnected to others through a combination of alternating current/high voltage direct current and thyristor control phase shifter in series with the tie-line. The interconnected power system is represented by state-space framework where phasor measurement units are used to obtain the system state information.
- The factor graph based state estimation algorithm is derived. It can compute the system states in a distributed way using the Bayesian graphical model.
- The effectiveness of the explored scheme is verified by extensive simulations.

The remainder of this paper is organized as follows. The interconnected power system model is presented in Section II. The propose estimation framework is in Section III, followed by the simulation results and discussions in Section IV.

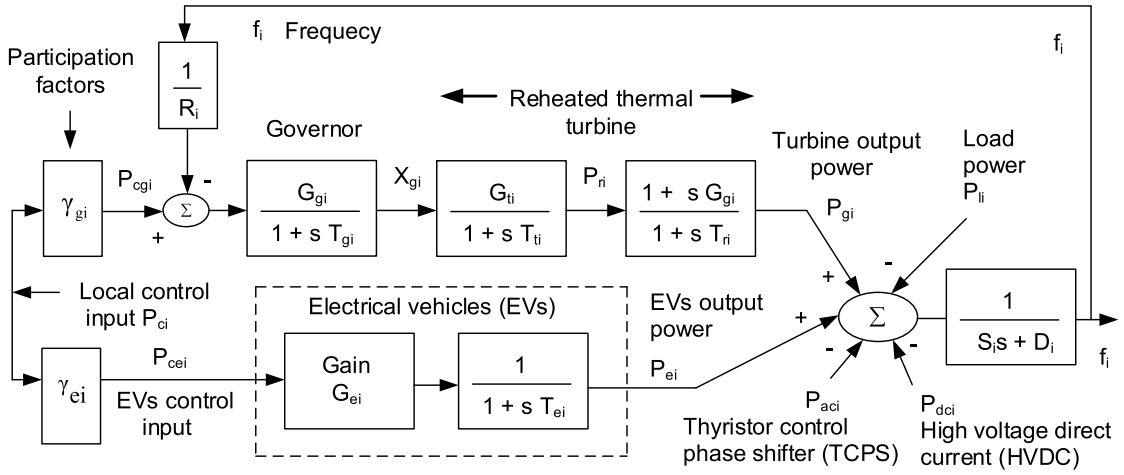

FIGURE 1. Transfer function of N-area interconnected power systems [3], [14].

Finally, the paper is wrapped up with conclusions and future work in Section V.

Notations: Usually, $N(\mathbf{x}, \mu, \mathbf{P})$ be the probability density function (PDF) of a Gaussian random variable $\mathbf{x}$ whose mean μ and covariance $\mathbf{P}$. Also PDF is expressed as $\pi_{\mathbf{x}(k-1),\mathbf{x}(k)}(\mathbf{x}(k-1)) = N(\mathbf{x}(k-1), \mathbf{x}_{\pi_{x(k-1)}}, \mathbf{\Sigma}_{\pi_{x(k-1)}})$ and $\pi_{\mathbf{x}(k-1)}(\mathbf{x}(k-1)) = N(\mathbf{x}(k-1), \hat{\mu}_{l(k-1)}, \mathbf{\Sigma}_{l(k-1)})$. The conditional probability is denoted by $p(\mathbf{x}(k) \mid \mathbf{x}(k-1)) = N(\mathbf{x}(k), \mathbf{A}_d\mathbf{x}(k-1) + \mathbf{B}_d\mathbf{u}(k-1), \mathbf{\Sigma}_n)$. The symbol diag(x) denotes the diagonal matrix with element x.

II. MULTI-AREA INTERCONNECTED POWER SYSTEMS

A mathematical model of an interconnected power system with turbines and electrical vehicles (EVs) is first derived. To illustrate, Fig. 1 shows the transfer function of N-area interconnected power systems [3], [14]. It can be seen that there are four main sections of this framework: dynamic model of EVs, plant with reheated thermal turbines, high voltage direct current (HVDC) links, and thyristor controlled phase shifter (TCPS) in the AC power tie-lines. In order to maintain the system frequency and power tie-line at the reference values, the control center sends the incremental change in power set-point of area i, P_{ci}, and through participation factors γ_{gi} and γ_{ei}, control signals P_{cgi} and P_{cei} are sent to regulate the output power of the generating units and EVs, respectively. The aggregator gathers information on all EVs and gives them to the control center. Furthermore, the aggregator obtains the power set-point from the control center and then allocates it to dispersed EVs. The fleet of EVs is modeled by a first-order with time constant T_{ei} and gain G_{ei} [15]–[18]. From the Fig. 1, the EVs output power deviation P_{ei} is given by:

$$P_{ei}(s) = \frac{G_{ei}}{1+sT_{ei}} P_{cei}(s). \tag{1}$$

Here, G_{ei} is the EVs gain, T_{ei} is the time constant and P_{cei} is the EVs control input.

In order to share HVDC links into LFC, the supplemental HVDC proportional controller is used. The HVDC power interchange P_{dci} is determined by the HVDC control signal ω_i with a time constant T_{dci} [19]–[21]. Generally, the ω_i signal is determined according to the difference between the frequency deviations of area i and the other areas j, $j = 1, 2, \cdots, N$, $j \neq i$ [22] with a HVDC gain G_{ij}. So, the interchange HVDC power P_{dci} is obtained by:

$$P_{dci}(s) = \frac{1}{1+sT_{dci}} \omega_i(s). \tag{2}$$

Here, the control signal $\omega_i(s) = \sum_{j=1,j\neq i}^{N} G_{ij}[f_i(s) - f_j(s)]$ and f_i is the frequency deviation at the area i.

The AC power tie-line deviation between area i and area j $P_{ac,ij}$ without TCPS is given by [14]:

$$P_{ac,ij}(s) = \frac{2\pi}{s} T_{ij}[f_i(s) - f_j(s)]. \tag{3}$$

Here, T_{ij} is the tie-line synchronizing coefficient. Moreover, the AC power tie-line deviation between area i and area j with TCPS is given by [23]:

$$P_{ac,ij}(s) = \frac{2\pi}{s} T_{ij}[f_i(s) - f_j(s) + P_{sij}(s)]. \tag{4}$$

Here, P_{sij} is the TCPS power deviation, and it is given by [3]:

$$\mathbf{P}_{sij}(s) = \frac{T_{ij}K_{sij}f_i(s)}{1+sT_{sij}}. \tag{5}$$

The AC tie-line power interchange deviation $\mathbf{P}_{aci}$ at area i is determined by:

$$\mathbf{P}_{aci}(s) = \sum_{j=1,j\neq i}^{N} P_{ac,ij}(s). \tag{6}$$

When there are load disturbances in LFC, it requires to maintain zero steady-state error for tie-line powers and frequencies. Basically, the *area control error (ACE)* is the

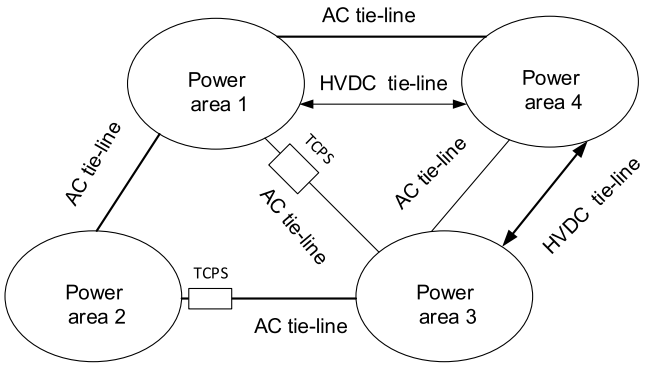

FIGURE 2. Topology of a four-area interconnected power system [3], [14].

difference between scheduled and actual electrical generations within a control area on the power grid, taking frequency bias into account. The ACE is determined according to the following expression:

$$ACE_i(t) = P_{tie,i}(t) + b_i f_i(t), \tag{7}$$

where, $P_{tie,i}(t) = P_{aci}(t) + P_{dci}(t)$ is the tie-line power interchange deviation at area i and b_i is the frequency bias constant.

The state-space representation for each area i of the interconnected power system is described as follows:

$$\dot{\mathbf{x}}_i(t) = \mathbf{A}_{ii}\mathbf{x}_i(t) + \sum_{j=1, j\neq i}^{N} \mathbf{A}_{ij}\mathbf{x}_j(t) + \mathbf{B}_i u_i(t) + \mathbf{D}_i d_i, \quad i = 1, 2, \cdots, N. \tag{8}$$

Here, the system state variable at area i $\mathbf{x}_i \in \mathbb{R}^{n_i} = [f_i X_{gi} P_{ri} P_{gi} P_{ei} \int ACE_i dt P_{tie,i} P_{dci} P_{sij}]'$, X_{gi} is the incremental change in governor valve position, the input signal $u_i = P_{ci}$, the load disturbance $d_i = P_{li}$ and P_l is load demand. The system state matrix $\mathbf{A}_{ii/ij}$, input matrix $\mathbf{B}_i$ and disturbance matrix $\mathbf{D}_i$ are derived in Appendix A. For simplicity, it assumes that there are four-area interconnected power systems whose topology is described in Fig. 2. It can be seen that the each area is interconnected to others through tie-line. Based on the above system equations, the interconnected power system is expressed as a linearized continuous-time state-space model as follows:

$$\dot{\mathbf{x}}(t) = \mathbf{A}\mathbf{x}(t) + \mathbf{B}\mathbf{u}(t) + \mathbf{D}\mathbf{d}(t). \tag{9}$$

Here, $\mathbf{x}(t) \in \mathbb{R}^{31}$ is the global state vector of the four-area interconnected power system, $\mathbf{u}(t) \in \mathbb{R}^4$ is the control effort and $\mathbf{d}(t) \in \mathbb{R}^4$ is the load disturbance. Specifically, the variable $\mathbf{x}(t)$ comprises four local areas state vectors, i.e., $\mathbf{x}(t) = [\mathbf{x}_1'(t)\mathbf{x}_2'(t)\mathbf{x}_3'(t)\mathbf{x}_4'(t)]'$. Similarly, $\mathbf{u}(t) = [P_{c1}(t)P_{c2}(t)P_{c3}(t)P_{c4}(t)]'$ and $\mathbf{d}(t) = [P_{l1}(t)P_{l2}(t)P_{l3}(t)P_{l4}(t)]'$. Moreover, the local state vector for each area, $\mathbf{x}_i(t)$ is defined as $\mathbf{x}_i(t) = [\mathbf{x}_{i1}'(t)\mathbf{x}_{i2}'(t)]'$, where $\mathbf{x}_{i1}(t) = [f_i(t)X_{gi}(t)P_{ri}(t)P_{gi}(t)P_{ei}(t) \int ACE_i(t)dt]'$ and $\mathbf{x}_{i2}(t)$ is defined as $\mathbf{x}_{12}(t) = [P_{tie,1}(t)P_{dc1}(t)P_{s13}(t)]'$, $\mathbf{x}_{22}(t) = [P_{tie,2}(t)P_{s23}(t)]'$, $\mathbf{x}_{32}(t) = [P_{tie,3}(t)P_{dc3}(t)]'$ and $\mathbf{x}_{42}(t) = [\emptyset]$, where $\emptyset$ is the empty set. Finally, the system input matrix $\mathbf{B} = diag(\mathbf{B}_1, \mathbf{B}_2, \mathbf{B}_3, \mathbf{B}_4)$, the disturbance matrix $\mathbf{D} = diag(\mathbf{D}_1, \mathbf{D}_2, \mathbf{D}_3, \mathbf{D}_4)$ and the system state matrix is given by:

$$\mathbf{A} = \begin{bmatrix} \mathbf{A}_{11} & \mathbf{A}_{12} & \mathbf{A}_{13} & \mathbf{A}_{14} \\ \mathbf{A}_{21} & \mathbf{A}_{22} & \mathbf{A}_{23} & \mathbf{A}_{24} \\ \mathbf{A}_{31} & \mathbf{A}_{32} & \mathbf{A}_{33} & \mathbf{A}_{34} \\ \mathbf{A}_{41} & \mathbf{A}_{42} & \mathbf{A}_{43} & \mathbf{A}_{44} \end{bmatrix}.$$

All the system matrices $\mathbf{A} \in \mathbb{R}^{31\times31}$, $\mathbf{B} \in \mathbb{R}^{31\times4}$ and $\mathbf{D} \in \mathbb{R}^{31\times4}$ are described in [3].

When the load disturbance is a step change of any magnitude, $\mathbf{d}(t)$ can be ignored in the design of state observers [3]. Similar to [3], [7], [24], and [25], this paper does not consider $\mathbf{d}(t)$, and the above system is expressed as a discrete-time state-space linear model as follows:

$$\mathbf{x}(k+1) = \mathbf{A}_d\mathbf{x}(k) + \mathbf{B}_d\mathbf{u}(k) + \mathbf{n}(k), \tag{10}$$

where $\mathbf{A}_d = \mathbf{I} + \mathbf{A}\Delta t$, $\mathbf{I}$ is the identity matrix, Δt is the sampling period, $\mathbf{B}_d = \mathbf{B}\Delta t$ and $\mathbf{n}(k)$ is the process uncertainties with covariance $\mathbf{\Sigma}_{\boldsymbol{n}}$.

In order to facilitate the two-way communication between power distribution system and utilities, the utility company uses phasor measurement units to monitor the grid. The observations from the grid are obtained by:

$$\mathbf{y}(k) = \mathbf{C}\mathbf{x}(k) + \mathbf{w}(k), \tag{11}$$

where $\mathbf{y}$ is the measurement, $\mathbf{C}$ is the sensing matrix and $\mathbf{w}$ is the zero mean Gaussian process noise whose covariance is $\mathbf{\Sigma}_{\boldsymbol{w}}$. The sensing information is transmitted to the energy management systems, where the state estimation is performed.

III. PROPOSED ESTIMATION ALGORITHM

The factor graph is a distributed message passing algorithm to achieve the global inference on graphical models. In this graph, the messages are probabilities which represent the level of belief about the value of system states [26], [27]. It consists of function nodes and variable nodes, where the information is propagated between them to obtain a reliable estimation [12], [28], [30]. The scheme works by passing real valued functions called messages along the edges between the nodes [26]. In this graph, the prior information π and likelihood λ are the messages sent to the virtual node x from its parents $(u_1, u_2, \ldots, u_m)$ and children $(y_1, y_2, \ldots, y_n)$, respectively [10], [29]. To illustrate, Fig. 3 shows the message passing in the factor graph [10], [29], [30]. The prior information passing from parents u_m to node x is $\pi_{u_m,x}(u_m)$, where $\pi_{u_m,x}(u_m)$ denotes the π message sent between u and x. The likelihood message passing from children y_n to node x is $\lambda_{y_n,x}(x)$. After x receiving all π messages $\pi_{u_m,x}(u_m)$ from its parents and all λ messages $\lambda_{y_n,x}(x)$ from its children, node x updates its state estimation. Then x transmits λ messages $\lambda_{x,u_m}(u_m)$ to its parents and π information $\pi_{x,y_n}(\mathbf{x})$ to its children [10], [29], [31]. The explicit message computation rules of the factor graph approach are given by [10], [29], [31]:

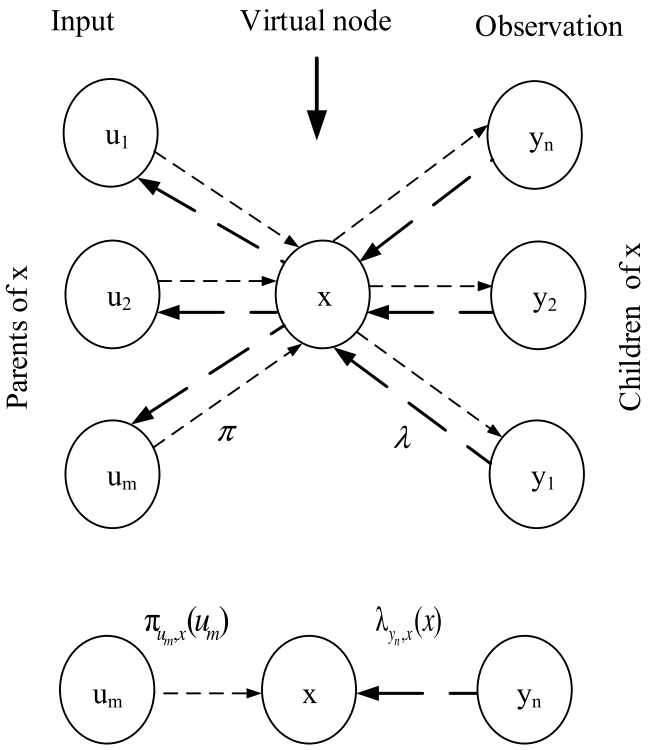

FIGURE 3. Information propagation [10], [30].

Message Update Rule 1: Combining the incoming messages $\pi_{u_m,x}$ from all parents $\mathbf{u} = (u_1, u_2, \ldots, u_m)$ into $\pi_x(\mathbf{x})$:

$$\pi_x(\mathbf{x}) = \sum_u p(\mathbf{x}|\mathbf{u}) \times \prod_{m=1}^{m} \pi_{u_m,x}(u_m). \tag{12}$$

Here, $p(\mathbf{x}|\mathbf{u})$ is the prior conditional probability.

Message Update Rule 2: Combining the incoming messages $\lambda_{y_n,x}$ from children $\mathbf{y} = (y_1, y_2, \ldots, y_n)$ into $\lambda_x(\mathbf{u})$:

$$\lambda_x(\mathbf{u}) = \sum_{\mathbf{x}} \prod_{n=1}^{n} \lambda_{y_n,x}(\mathbf{x}) \times p(\mathbf{x}|\mathbf{u}). \tag{13}$$

Message Update Rule 3: After x receiving all π messages $\pi_{u_m,x}(u_m)$ from its parents $(u_1, u_2, \ldots, u_m)$ and all λ messages $\lambda_{y_n,x}(x)$ from its children $(y_1, y_2, \ldots, y_n)$, node x updates its belief/state estimation $\hat{\mathbf{x}}_b$ by:

$$\hat{\mathbf{x}}_b = \alpha \times \prod_{n=1}^{n} \lambda_{y_n,x}(\mathbf{x}) \times \pi_x(\mathbf{x}). \tag{14}$$

Here, α is called a normalization constant which depends on application scenarios. This normalization may prevent numerical underflow problems or it uses to normalize a vector so that its elements sum to 1.

Message Update Rule 4: If $\pi_x(\mathbf{x})$ has been calculated and x receives all λ messages from its children (except y_i i.e., $i \neq n$), x calculates $\pi_{x,y_n}(\mathbf{x})$, then x transmits π messages to its children by:

$$\pi_{x,y_n}(\mathbf{x}) = \pi_x(\mathbf{x}) \times \prod_{i \neq n} \lambda_{y_i,x}(\mathbf{x}). \tag{15}$$

Message Update Rule 5: If $\lambda_x(\mathbf{u})$ has been computed and x receives all π messages from its parents (except u_j i.e.,$j \neq m$), x computes $\lambda_{x,u_m}(u_m)$, then x transmits λ messages to its parents by the following expression:

$$\lambda_{x,u_m}(u_m) = \sum_{\mathbf{u} \neq u_m} \lambda_x(\mathbf{u}) \times \prod_{j \neq m} \pi_{u_j,x}(u_j). \tag{16}$$

In the language of message passing algorithm, the message that a node delivers to a node should not be based on the information received from that node. In this algorithm, the system state information passes back and forward between the function and variable nodes to achieve the global inference. In order to run the message passing algorithm, the following initial value are used:

$$\lambda_{x,u}(\mathbf{u}) = \begin{cases} p(\mathbf{x}_0 \mid \mathbf{u}), & \text{x is evidence, } \mathbf{x} = \mathbf{x}_0, \\ 1, & \text{otherwise (no child).} \end{cases} \tag{17}$$

$$\pi_{x,y}(\mathbf{x}) = \begin{cases} \delta(\mathbf{x}, \mathbf{x}_0), & \text{x is evidence, } \mathbf{x} = \mathbf{x}_0, \\ p(\mathbf{x}), & \text{x is source.} \end{cases} \tag{18}$$

Here, $p(\mathbf{x})$ is the prior probability.

From the system state-space model and its measurement, it can be seen that the current system state dependent on the previous state and system input. Technically, the detailed pictorial view of messages exchange in three time slots during the state estimation process is depicted in Fig. 4 [10], [29], [30]. Based on the Bayesian structure, the asynchronous updating order and messages passing (forward, backward and smoothing) is as follows [10], [29]:

Step 1) $\mathbf{x}(k-1) \rightarrow \mathbf{y}(k-1)$; step 2) $\mathbf{y}(k-1) \rightarrow \mathbf{x}(k-1)$; step 3) $\mathbf{x}(k-1) \rightarrow \mathbf{x}(k)$; step 4) $\mathbf{x}(k) \rightarrow \mathbf{y}(k)$; step 5) $\mathbf{y}(k) \rightarrow \mathbf{x}(k)$; step 6) $\mathbf{x}(k) \rightarrow \mathbf{x}(k-1)$ and step 7) $\mathbf{x}(k-1)$ is the updated state estimation.

Here, $\mathbf{x}(k-1) \rightarrow \mathbf{y}(k-1)$ means that the message is updated and kept at node $\mathbf{x}(k-1)$. The step-by-step process of the proposed approach is described as follows [10], [29], [31]:

Forward Pass $\mathbf{x}(k-1) \rightarrow \mathbf{y}(k-1)$: Let's first apply the message passing *rule 1* to the function node $\mathbf{x}(k-1)$, so the prior information is written as follows:

$$\begin{aligned} \pi_{\mathbf{x}(k-1)}(\mathbf{x}(k-1)) &= \int_{-\infty}^{\infty} p(\mathbf{x}(k-1) \mid \mathbf{x}(k-2)) \\ &\quad \times \pi_{\mathbf{x}(k-2),\mathbf{x}(k-1)}(\mathbf{x}(k-2)) d\mathbf{x}(k-2) \\ &= p(\mathbf{x}(k-1)) = N(\mathbf{x}(k-1), \hat{\mu}_{l(k-1)}, \boldsymbol{\Sigma}_{l(k-1)}), \end{aligned}$$

where the mean $\hat{\mu}_{l(k-1)}$ and error covariance $\boldsymbol{\Sigma}_{l(k-1)}$ of $\mathbf{x}(k-1)$ come from Eq. (10) as follows [10], [29]:

$$\hat{\mu}_{l(k-1)} = \mathbf{A}_d \hat{\mathbf{x}}_{\pi_x(k-2)} + \mathbf{B}_d \mathbf{u}(k-1). \tag{19}$$

$$\boldsymbol{\Sigma}_{l(k-1)} = \mathbf{A} \boldsymbol{\Sigma}_{\pi_x(k-2)} \mathbf{A}_d' + \boldsymbol{\Sigma}_{\boldsymbol{n}}. \tag{20}$$

Here, $\hat{\mathbf{x}}_{\pi_x(k-2)}$ and $\boldsymbol{\Sigma}_{\pi_x(k-2)}$ are the initial mean and covariance from the previous time slot. After applying the updating *rule 5* in step $\mathbf{x}(k-1) \rightarrow \mathbf{y}(k-1)$, we have:

$$\begin{aligned} \pi_{\mathbf{x}(k-1),\mathbf{y}(k-1)}(\mathbf{x}(k-1)) &= \pi_{\mathbf{x}(k-1)}(\mathbf{x}(k-1)) \\ &\quad \times \lambda_{\mathbf{y}(k-1),\mathbf{x}(k-1)}(\mathbf{x}(k-1)). \end{aligned} \tag{21}$$

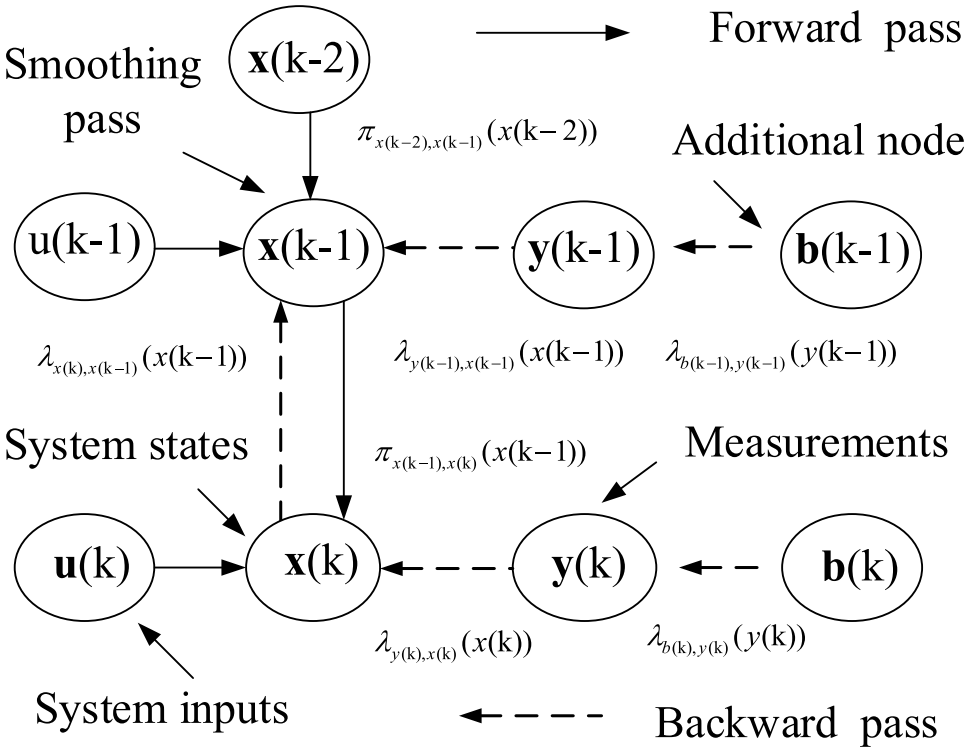

FIGURE 4. The system state estimation process [10], [30].

From the Fig. 4 and mentioned initial value in (17), it can be seen that $\lambda_{\mathbf{y}(k-1),\mathbf{x}(k-1)}(\mathbf{x}(k-1)) = 1$ as $\mathbf{y}(k-1)$ has no child nodes. So, (21) can be written as follows:

$$\begin{aligned}\pi_{\mathbf{x}(k-1),\mathbf{y}(k-1)}(\mathbf{x}(k-1)) &= \pi_{\mathbf{x}(k-1)}(\mathbf{x}(k-1)) = p(\mathbf{x}(k-1)) \\ &= N(\mathbf{x}(k-1), \hat{\mu}_{l(k-1)}, \boldsymbol{\Sigma}_{l(k-1)}) \\ &= N(\mathbf{x}(k-1), \hat{\mu}_{\pi_{y(k-1)}}, \boldsymbol{\Sigma}_{\pi_{y(k-1)}}),\end{aligned}$$

where

$$\hat{\mu}_{\pi_{y(k-1)}} = \hat{\mu}_{l(k-1)} = \mathbf{A}_d \hat{\mathbf{x}}_{\pi_x(k-2)} + \mathbf{B}_d \mathbf{u}(k-1). \quad (22)$$

$$\boldsymbol{\Sigma}_{\pi_{y(k-1)}} = \boldsymbol{\Sigma}_{l(k-1)} = \mathbf{A}\boldsymbol{\Sigma}_{\pi_x(k-2)}\mathbf{A}'_d + \boldsymbol{\Sigma}_{\boldsymbol{n}}. \quad (23)$$

Backward Pass $\mathbf{y}(k-1) \rightarrow \mathbf{x}(k-1)$: Let's apply the message passing *rule 2* to the variable node $\mathbf{y}(k-1)$, so the likelihood information is:

$$\begin{aligned}\lambda_{\mathbf{y}(k-1)}(\mathbf{x}(k-1)) = \int_{-\infty}^{\infty} &\pi_{\mathbf{b}(k-1),\mathbf{y}(k-1)}(\mathbf{y}(k-1)) \\ &\times p(\mathbf{y}(k-1) \mid \mathbf{x}(k-1)) d\mathbf{y}(k-1). \quad (24)\end{aligned}$$

Here, we add an additional node $\mathbf{b}(k-1)$ in Fig. 4 as there is no transferring information from the childless node $\mathbf{y}(k-1)$ to other. The parent node is there, but it is not considered for transferring the information according to the message passing *rule 5*. In other words, the information that a node delivers to a node should not be based on the message received from that node. So, the term $\pi_{\mathbf{b}(k-1),\mathbf{y}(k-1)}$ is just used to describe the process. Now (24) can be written as follows:

$$\lambda_{\mathbf{y}(k-1)}(\mathbf{x}(k-1)) = N(\mathbf{x}(k-1), \hat{\mu}_{\lambda_y(k-1)}, \boldsymbol{\Sigma}_{\lambda_y(k-1)}), \quad (25)$$

where the mean and error covariance are given by:

$$\hat{\mu}_{\lambda_y(k-1)} = \mathbf{C}^{-1}\mathbf{y}_{\lambda_y(k-1)}. \quad (26)$$

$$\boldsymbol{\Sigma}_{\lambda_y(k-1)} = \mathbf{C}^{-1}\boldsymbol{\Sigma}_{\boldsymbol{w}}\mathbf{C}'^{-1}. \quad (27)$$

The observation information $\mathbf{y}(k-1)$ is same as $\mathbf{y}_{\lambda_y(k-1)}$, which uses to maintain the notational consistency of the backward information propagation. Similar to the step 1 and after applying the *rule 5* to the variable node $\mathbf{y}(k-1)$, it can be be seen that $\lambda_{\mathbf{y}(k-1)}(\mathbf{x}(k-1)) = \lambda_{\mathbf{y}(k-1),\mathbf{x}(k-1)}(\mathbf{x}(k-1))$. This means that the combing incoming child messages to the virtual node and its updated information is same.

Lemma 1: Let $N(\mathbf{x}, \mu_1, \mathbf{P}_1)$ and $N(\mathbf{x}, \mu_2, \mathbf{P}_2)$ be the probability density functions of a Gaussian random variable $\mathbf{x}$, then their product is another Gaussian variable as follows:

$$N(\mathbf{x}, \mu_1, \mathbf{P}_1)N(\mathbf{x}, \mu_2, \mathbf{P}_2) \propto N(\mathbf{x}, \mu, \mathbf{P}),$$

where the mean and covariance are given by [32]:

$$\mu = \mathbf{P}^{-1}[\mathbf{P}_1\mu_1 + \mathbf{P}_2\mu_2].$$
$$\mathbf{P}^{-1} = (\mathbf{P}_1 + \mathbf{P}_2)^{-1}.$$

Proof: See [32] Lemma 12 and it's derivation.

Smoothing Pass $\mathbf{x}(k-1) \rightarrow \mathbf{x}(k)$**:** This step is considered as a preliminary estimation due to the fact that the initial values are assumed for previously developed expressions. After x receiving priori information from step 1 and likelihood messages from step 2, node x updates its state information according to the message passing *rule 3*. Using

Lemma 1, the term $\pi_{\mathbf{x}(k-1),\mathbf{x}(k)}(\mathbf{x}(k-1))$ can express as follows [10], [29]:

$$\begin{aligned}\pi_{\mathbf{x}(k-1),\mathbf{x}(k)}(\mathbf{x}(k-1)) &= \pi_{\mathbf{x}(k-1)}(\mathbf{x}(k-1))\lambda_{\mathbf{y}(k-1),\mathbf{x}(k-1)} \\ &\quad \times(\mathbf{x}(k-1)) \\ &= N(\mathbf{x}(k-1), \hat{\mu}_{\pi_x(k-1)}, \mathbf{\Sigma}_{\pi_x(k-1)}),\end{aligned}$$

where the mean and error covariance are computed as follows:

$$\begin{aligned}\hat{\mu}_{\pi_x(k-1)} &= \mathbf{\Sigma}_{\pi_x(k-1)}[\mathbf{\Sigma^{-1}}_{l(k-1)} \times \hat{\mu}_{l(k-1)} + \mathbf{\Sigma}_{\lambda_y(k-1)} \\ &\quad \times \hat{\mu}_{\lambda_y(k-1)}]. \qquad (28)\\ \mathbf{\Sigma}_{\pi_x(k-1)} &= [\mathbf{\Sigma^{-1}}_{l(k-1)} + \mathbf{\Sigma}_{\lambda_y(k-1)}]^{-1}. \qquad (29)\end{aligned}$$

After applying the message passing *rule 3* with $\alpha = 1$, the preliminary state estimation is determined by:

$$\begin{aligned}\hat{\mathbf{x}}(k-1) &= 1 \times \lambda_{\mathbf{y}(k-1),\mathbf{x}(k-1)}(\mathbf{x}(k-1))\pi_{\mathbf{x}(k-1)}(\mathbf{x}(k-1)) \\ &= N(\mathbf{x}(k-1), \hat{\mu}_{b(k-1)}, \mathbf{\Sigma}_{b(k-1)}), \qquad (30)\end{aligned}$$

where the mean and covariance are computed as follows:

$$\begin{aligned}\hat{\mu}_{b(k-1)} &= \mathbf{\Sigma}_{b(k-1)}[\mathbf{\Sigma^{-1}}_{l(k-1)} \times \hat{\mu}_{l(k-1)} \\ &\quad + \mathbf{\Sigma}_{\lambda_y(k-1)}\hat{\mu}_{\lambda_y(k-1)}]. \qquad (31)\\ \mathbf{\Sigma}_{b(k-1)} &= [\mathbf{\Sigma^{-1}}_{l(k-1)} + \mathbf{\Sigma}_{\lambda_y(k-1)}]^{-1}. \qquad (32)\end{aligned}$$

This updated information is kept at time slot k-1, so it requires to update the system states at k as shown in Fig. 4. Obviously, it can be perceived that the step 4 and 5 are similar to the step 1 and 2, respectively where corresponding inputs/outputs come from the sequence of message flows.

Forward Pass $\mathbf{x}(k) \rightarrow \mathbf{y}(k)$: Similar to the forward message passing in step 1, the updated information for step 4 is given by:

$$\pi_{\mathbf{x}(k),\mathbf{y}(k)}(\mathbf{x}(k)) = N(\mathbf{x}(k), \hat{\mu}_{\pi_{y(k)}}, \mathbf{\Sigma}_{\pi_{y(k)}}),$$

with

$$\begin{aligned}\hat{\mu}_{\pi_{y(k)}} &= \mathbf{A}_d\hat{\mu}_{b(k-1)} + \mathbf{B}_d\mathbf{u}(k). \qquad (33)\\ \mathbf{\Sigma}_{\pi_{y(k)}} &= \mathbf{A}\mathbf{\Sigma}_{b(k-1)}\mathbf{A}'_d + \mathbf{\Sigma}_{\boldsymbol{n}}. \qquad (34)\end{aligned}$$

Backward Pass $\mathbf{y}(k) \rightarrow \mathbf{x}(k)$ and $\mathbf{x}(k) \rightarrow \mathbf{x}(k-1)$: Similar to the backward step 2, the updated information for step 5 is given by:

$$\lambda_{\mathbf{y}(k),\mathbf{x}(k)}(\mathbf{x}(k)) = N(\mathbf{x}(k), \hat{\mu}_{\lambda_y(k)}, \mathbf{\Sigma}_{\lambda_y(k)}),$$

with

$$\begin{aligned}\hat{\mu}_{\lambda_y(k)} &= \mathbf{C}^{-1}\mathbf{y}_{\lambda_y(k)}. \qquad (35)\\ \mathbf{\Sigma}_{\lambda_y(k)} &= \mathbf{C}^{-1}\mathbf{\Sigma}_{\boldsymbol{w}}\mathbf{C}'^{-1}. \qquad (36)\end{aligned}$$

For the backward step $\mathbf{x}(k) \rightarrow \mathbf{x}(k-1)$, we have:

$$\begin{aligned}\lambda_{\mathbf{x}(k)}(\mathbf{x}(k-1)) &= \int_{-\infty}^{\infty} \lambda_{\mathbf{y}(k),\mathbf{x}(k)}(\mathbf{x}(k))p(\mathbf{x}(k)\,|\,\mathbf{x}(k-1))d\mathbf{x}(k) \\ &= N(\mathbf{x}(k), \hat{\mu}_{\lambda_y(k)}, \mathbf{\Sigma}_{\lambda_y(k)})p(\mathbf{x}(k)|\,\mathbf{x}(k-1))d\mathbf{x}(k) \\ &= N(\mathbf{x}(k-1), \hat{\mu}_{\lambda_y(k-1)}, \mathbf{\Sigma}_{\lambda_y,(k-1)}),\end{aligned}$$

where the mean and covariance are determined as follows:

$$\begin{aligned}\hat{\mu}_{\lambda_y(k-1)} &= \mathbf{A}_d^{-1}\hat{\mu}_{\lambda_y(k)} - \mathbf{A}_d^{-1}\mathbf{B}_d\mathbf{u}(k). \qquad (37)\\ \mathbf{\Sigma}_{\lambda_y(k-1)} &= \mathbf{A}_d^{-1}(\mathbf{\Sigma}_{\lambda_y(k)} + \mathbf{\Sigma}_{\boldsymbol{n}})\mathbf{A}_d'^{-1}. \qquad (38)\end{aligned}$$

Updated State Estimation: From the Fig. 4, it can be seen that after information obtaining from the step 1, 2, and 6, the node $\mathbf{x}(k-1)$ is updated it estimations. Similar to the step 5, the final estimated state $\hat{\mathbf{x}}_b(k-1)$ is computed by [10], [29]:

$$\begin{aligned}\hat{\mathbf{x}}_b(k-1) &= 1 \times \lambda_{\mathbf{x}(k),\mathbf{x}(k-1)}(\mathbf{x}(k-1))\lambda_{\mathbf{y}(k-1),\mathbf{x}(k-1)} \\ &\quad (\mathbf{x}(k-1))\pi_{\mathbf{x}(k-1)}(\mathbf{x}(k-1)) \\ &= N(\mathbf{x}(k-1), \hat{\mu}_{b(k-1)}, \mathbf{\Sigma}_{b(k-1)}), \qquad (39)\end{aligned}$$

where the estimated state and its error covariance are:

$$\begin{aligned}\hat{\mu}_{b(k-1)} &= \mathbf{\Sigma}_{b(k-1)}[\mathbf{\Sigma^{-1}}_{\lambda_y(k-1)} \times \hat{\mu}_{\lambda_y(k-1)} + \mathbf{\Sigma^{-1}}_{l(k-1)} \\ &\quad \times \hat{\mu}_{l(k-1)} + \mathbf{\Sigma^{-1}}_{\lambda_x(k-1)} \times \hat{\mu}_{\lambda_x(k-1)}]. \qquad (40)\\ \mathbf{\Sigma}_{b(k-1)} &= [\mathbf{\Sigma^{-1}}_{\lambda_y(k-1)} + \mathbf{\Sigma^{-1}}_{l(k-1)} + \mathbf{\Sigma^{-1}}_{\lambda_x(k-1)}]^{-1}. \\ &\qquad (41)\end{aligned}$$

Basically, in each step the proposed algorithm locally passes information from one node to their associated next nodes and vice-versa.

IV. SIMULATION RESULTS AND DISCUSSIONS

The simulation parameters for interconnected power systems are shown in Table 1, where Matlab is used as tool [3], [14], [33]. From the simulation results as shown in Figs. 5-7, it can be seen that the proposed algorithm can be

TABLE 1. System parameters for interconnected power systems [3], [14], [33].

Parameters	Values	Parameters	Values	Parameters	Values
T_{ti}	0.3	G_{ti}	1	G_{ri}	0.5
T_{ri}	10	R_i	2.4	S_i	0.1667
T_{ei}	1	b_i	0.4250	η_{gi}	0.9
η_{ei}	0.1	$G_{s13/s23}$	1	$T_{s12/s23}$	0.1
D_i	0.0083	$T_{ij/ji}$	0.026	$G_{14/43}$	0.1
G_{gi}	1	Δt	0.03 sec	T_{gi}	0.08
$\mathbf{\Sigma_n}$	0.001*$\mathbf{I}$	$\mathbf{\Sigma_w}$	0.01*$\mathbf{I}$	$T_{dc1/dc3}$	0.2

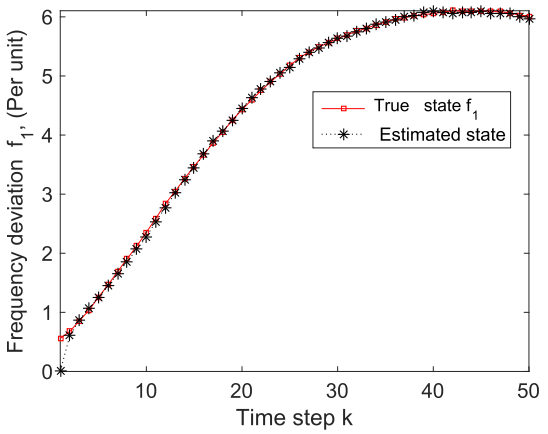

FIGURE 5. Frequency deviation f_1 and its estimate for area 1.

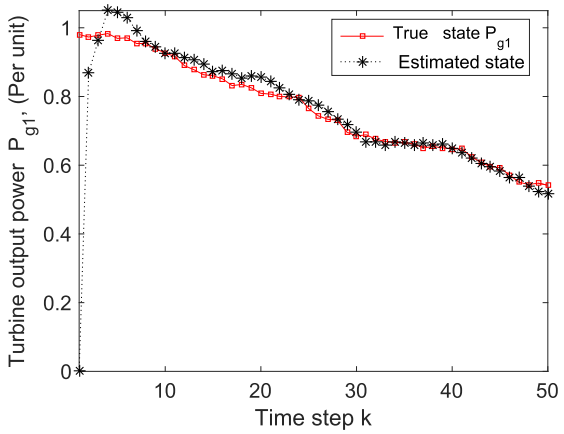

FIGURE 6. Turbine output power P_{g1} and its estimate for area 1.

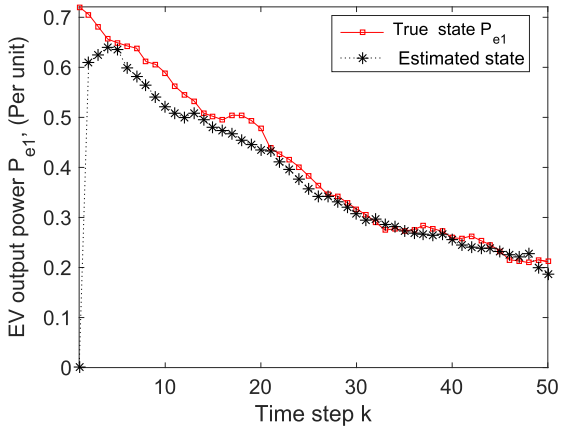

FIGURE 7. EV output power P_{e1} and its estimate for area 1.

well estimated the system states within 0.9 seconds ($k \times \Delta_t$). This is due to the fact that the estimation errors are rectified in a distributed way considering the Bayesian network. Other states have similar estimation accuracy, so they are omitted.

V. CONCLUSION AND FUTURE WORK

This paper presents a state-space model for interconnected power systems incorporating turbine and electrical vehicle dynamic models. A state estimation algorithm is derived based on the factor graph and Bayesian structures. The designed scheme can be perfectly estimated the system states in a distributed way using the Bayesian framework. Simulation results show that the developed schemes can be well estimated the system states in a fairly short time. The future work involves the convergence analysis of the developed scheme.

REFERENCES

[1] T. N. Pham, S. Nahavandi, L. Van Hien, H. Trinh, and K. P. Wong, "Static output feedback frequency stabilization of time-delay power systems with coordinated electric vehicles state of charge control," *IEEE Trans. Power Syst.*, vol. 32, no. 5, pp. 3862–3874, Sep. 2017.

[2] H. A. Yousef, K. Al-Kharusi, M. H. Albadi, and N. Hosseinzadeh, "Load frequency control of a multi-area power system: An adaptive fuzzy logic approach," *IEEE Trans. Power Syst.*, vol. 29, no. 4, pp. 1822–1830, Jul. 2014.

[3] T. N. Pham, H. Trinh, and L. Van Hien, "Load frequency control of power systems with electric vehicles and diverse transmission links using distributed functional observers," *IEEE Trans. Smart Grid*, vol. 7, no. 1, pp. 238–252, Jan. 2016.

[4] A. K. Singh, R. Singh, and B. C. Pal, "Stability analysis of networked control in smart grids," *IEEE Trans. Smart Grid*, vol. 6, no. 1, pp. 381–390, Jan. 2015.

[5] J. Schiffer, D. Zonetti, R. Ortega, A. M. Stanković, T. Sezi, and J. Raisch, "A survey on modeling of microgrids—From fundamental physics to phasors and voltage sources," *Automatica*, vol. 74, pp. 135–150, Dec. 2016.

[6] G. Pillonetto, B. M. Bell, and S. D. Favero, "Distributed Kalman smoothing in static Bayesian networks," *Automatica*, vol. 49, no. 4, pp. 1001–1011, 2013.

[7] H. Trinh, T. Fernando, H. H. C. Iu, and K. P. Wong, "Quasi-decentralized functional observers for the LFC of interconnected power systems," *IEEE Trans. Power Syst.*, vol. 28, no. 3, pp. 3513–3514, Aug. 2013.

[8] A. Sargolzaei, K. K. Yen, and M. N. Abdelghani, "Preventing time-delay switch attack on load frequency control in distributed power systems," *IEEE Trans. Smart Grid*, vol. 7, no. 2, pp. 1176–1185, Mar. 2016.

[9] E. E. Ejegi, J. A. Rossiter, and P. Trodden, "Distributed model predictive load frequency control of a deregulated power system," in *Proc. 11th Int. Conf. Control*, Aug./Sep. 2016, pp. 1–6.

[10] S. Gong, H. Li, L. Lai, and R. C. Qiu, "Decoding the 'nature encoded' messages for distributed energy generation control in microgrid," in *Proc. Int. Conf. Commun.*, Jun. 2011, pp. 1–5.

[11] P. Chavali and A. Nehorai, "Distributed power system state estimation using factor graphs," *IEEE Trans. Signal Process.*, vol. 63, no. 11, pp. 2864–2876, Jun. 2015.

[12] Y. Hu, A. Kuh, T. Yang, and A. Kavcic, "A belief propagation based power distribution system state estimator," *IEEE Comput. Intell. Mag.*, vol. 6, no. 3, pp. 36–46, Aug. 2011.

[13] Y. Li, "Fully distributed state estimation of smart grids," in *Proc. Int. Conf. Commun.*, Jun. 2012, pp. 6580–6585.

[14] C. E. Fosha and O. I. Elgerd, "The megawatt-frequency control problem: A new approach via optimal control theory," *IEEE Trans. Power App. Syst.*, vol. PAS-89, no. 4, pp. 563–577, Apr. 1970.

[15] H. Liu, Z. Hu, Y. Song, and J. Lin, "Decentralized vehicle-to-grid control for primary frequency regulation considering charging demands," *IEEE Trans. Power Syst.*, vol. 28, no. 3, pp. 3480–3489, Aug. 2013.

[16] Y. Mu, J. Wu, J. Ekanayake, N. Jenkins, and H. Jia, "Primary frequency response from electric vehicles in the great britain power system," *IEEE Trans. Smart Grid*, vol. 4, no. 2, pp. 1142–1150, Jun. 2013.

[17] Y. Ota, H. Taniguchi, T. Nakajima, K. M. Liyanage, J. Baba, and A. Yokoyama, "Autonomous distributed V2G (vehicle-to-grid) satisfying scheduled charging," *IEEE Trans. Smart Grid*, vol. 3, no. 1, pp. 559–564, Mar. 2012.

[18] S. Vachirasricirikul and I. Ngamroo, "Robust LFC in a smart grid with wind power penetration by coordinated V2G control and frequency controller," *IEEE Trans. Smart Grid*, vol. 5, no. 1, pp. 371–380, Jan. 2014.

[19] Ibraheem, Nizamuddin, and T. S. Bhatti, "AGC of two area power system interconnected by AC/DC links with diverse sources in each area," *Int. J. Elect. Power Energy Syst.*, vol. 55, pp. 297–304, Feb. 2014.

[20] E. Rakhshani, A. Luna, K. Rouzbehi, P. Rodriguez, and I. Etxeberria-Otadui, "Effect of VSC-HVDC on load frequency control in multi-area power system," in *Proc. Energy Convers. Congr. Expo.*, Sep. 2012, pp. 4432–4436.

[21] N. Rostamkolai *et al.*, "Control design of Santo tome back-to-back HVDC link," *IEEE Trans. Power Syst.*, vol. 8, no. 3, pp. 1250–1256, Aug. 1993.

[22] J. Dai, Y. Phulpin, A. Sarlette, and D. Ernst, "Coordinated primary frequency control among non-synchronous systems connected by a multi-terminal high-voltage direct current grid," *IET Gener., Transmiss. Distrib.*, vol. 6, no. 2, pp. 99–108, Feb. 2012.

[23] R. J. Abraham, D. Das, and A. Patra, "Effect of TCPS on oscillations in tie-power and area frequencies in an interconnected hydrothermal power system," *IET Gener., Transmiss. Distrib.*, vol. 1, no. 4, pp. 632–639, Jul. 2007.

[24] K. Yamashita and T. Taniguchi, "Optimal observer design for load-frequency control," *Int. J. Elect. Power Energy Syst.*, vol. 8, no. 2, pp. 93–100, 1986.

[25] M. Aldeen and J. F. Marsh, "Decentralised proportional-plus-integral design method for interconnected power systems," *IEE Proc. C-Gener., Transmiss. Distrib.*, vol. 138, no. 4, pp. 263–274, Jul. 1991.

[26] F. R. Kschischang, B. J. Frey, and H.-A. Loeliger, "Factor graphs and the sum-product algorithm," *IEEE Trans. Inf. Theory*, vol. 47, no. 2, pp. 498–519, Feb. 2001.
[27] H.-A. Loeliger, J. Dauwels, J. Hu, S. Korl, L. Ping, and F. R. Kschischang, "The factor graph approach to model-based signal processing," *Proc. IEEE*, vol. 95, no. 6, pp. 1295–1322, Jun. 2007.
[28] Y. Hu, A. Kuh, A. Kavcic, and D. Nakafuji, "Real-time state estimation on micro-grids," in *Proc. Int. Joint Conf. Neural Netw.*, Jul./Aug. 2011, pp. 1378–1385.
[29] J. Pearl, *Probabilistic Reasoning in Intelligent Systems: Networks of Plausible Inference*. San Mateo, CA, USA: Morgan Kaufmann, 1988.
[30] M. M. Rana, W. Xiang, and E. Wang, "Smart grid state estimation and stabilisation," *Int. J. Elect. Power Energy Syst.*, vol. 102, pp. 152–159, Nov. 2018.
[31] B. S. Ruffer, C. M. Kellett, P. M. Dower, and S. R. Weller, "Belief propagation as a dynamical system: The linear case and open problems," *IET Control Theory Appl.*, vol. 4, no. 7, pp. 1188–1200, Jul. 2010.
[32] D. Bickson. (2008). "Gaussian belief propagation: Theory and aplication." [Online]. Available: https://arxiv.org/abs/0811.2518
[33] S. Xu and J. Lam, *Robust Control and Filtering of Singular Systems*. New York, NY, USA: Springer, 2006.

MD M. RANA, photograph and biography not available at the time of publication.

WEI XIANG (S'00–M'04–SM'10) received the B.Eng. and M.Eng. degrees in electronic engineering from the University of Electronic Science and Technology of China, Chengdu, China, in 1997 and 2000, respectively, and the Ph.D. degree in telecommunications engineering from the University of South Australia, Adelaide, Australia, in 2004.

From 2004 to 2015, he was with the School of Mechanical and Electrical Engineering, University of Southern Queensland, Toowoomba, Australia. He is currently the Founding Professor and the Head of Discipline of Internet of Things Engineering, James Cook University, Cairns, Australia. He has published over 250 peer-reviewed papers with over 100 IEEE journal articles. His research interest falls under the broad areas of communications and information theory, particularly the Internet of Things, and coding and signal processing for multimedia communications systems. He is an Elected Fellow of the IET and Engineers Australia. He was named a Queensland International Fellow (2010–2011) by the Queensland Government of Australia, an Endeavour Research Fellow (2012–2013) by the Commonwealth Government of Australia, a Smart Futures Fellow (2012–2015) by the Queensland Government of Australia, and a JSPS Invitational Fellow jointly by the Australian Academy of Science and Japanese Society for Promotion of Science (2014–2015). He received the TNQ Innovation Award in 2016, the Pearcey Entrepreneurship Award (Highly Commended) in 2017, and Engineers Australia Cairns Engineer of the Year in 2017. He was a co-recipient of three Best Paper Awards at 2015 WCSP, 2011 IEEE WCNC, and 2009 ICWMC. He has been awarded several prestigious fellowship titles. He is the Vice Chair of the IEEE Northern Australia Section. He has severed in a large number of international conferences in the capacity of a General Co-Chair, a TPC Co-Chair, and a Symposium Chair. He was an Editor for the IEEE COMMUNICATIONS LETTERS (2015–2017), and is an Associate Editor for Springer's *Telecommunications Systems*.

ERIC (GENGKUN) WANG received the B.Eng. degree in mechanical engineering and the M.Eng. degree in mechatronic engineering from the University of Science and Technology, Beijing, China, in 2006 and 2009, respectively, and the Ph.D. degree in telecommunications engineering from the University of South Queensland (USQ), Toowoomba, QLD, Australia. He was a Post-Doctoral Research Fellow with the School of Electrical and Mechanical, USQ, for two and half years. He is currently a Lecturer with James Cook University, Cairns, Australia. He has authored over 20 high quality papers, and participated in many national and international research projects. He was the runner-up in The Asia-Pacific Robot Contest (ABU Robocon) 2006. He received the Best Paper Award from the IEEE Wireless Communications and Networking Conference, Cancun, Mexico, in 2011.

XUEHUA LI received the Ph.D. degree in telecommunications engineering from the Beijing University of Posts and Telecommunications, Beijing, China, in 2008. She is currently a Professor and the Deputy Dean of the School of Information and Communication Engineering, Beijing Information Science and Technology University, China. She is also a Senior Member of the Beijing Internet of Things Institute. Her research interests are in the broad areas of communications and information theory, particularly the Internet of Things, and coding for multimedia communications systems.